ISSN 1064-2307, Journal of Computer and Systems Sciences International, 2010, Vol. 49, No. 1, pp. 144–151. © Pleiades Publishing, Ltd., 2010.
Original Russian Text © K.A. Sapronov, A.A. Cherepanov, S.F. Yatsun, 2010, published in Izvestiya Akademii Nauk. Teoriya i Sistemy Upravleniya, 2010, No. 1, pp. 147–155.

ROBOTICS

Investigation of Motion of a Mobile Two-Mass Vibration-Driven System

K. A. Sapronov, A. A. Cherepanov, and S. F. Yatsun

Kursk State Technical University, ul. 50 Let Oktyabrya, 94, Kursk, 305040 Russia

Received May 28, 2009

Abstract—The mathematical model of a mobile vibration-driven system consisting of two solid bodies connected by the piecewise linear viscous–elastic element and the electromagnetic drive is considered. The system moves along a rough surface using friction asymmetry at the mass–surface contact. Both shock-free and shock modes of motion are considered, dependences of the average velocity of translational motion of the system on the frequency of the external periodic control voltage are obtained.

DOI: 10.1134/S1064230710010156

INTRODUCTION

Mobile devices which can move without special movers interacting with the environment directly by their frame possess a number of advantages, as compared to wheeled, crawling, and walking systems first of all due to the simple design. This advantage allows one to use these principles to create miniature microrobots capable of moving in narrow channels, slits, and environments inaccessible for other mobile objects.

A large cycle of papers [1–12] is devoted to devices which represent a chain of rigid links connected by rotary joints in which drives are situated. These drives create control moments internal for the multi-link robot. Dry friction acts between the multi-link robot and the surface along which it moves. By controlling the moments at the joints, and thus, the friction force applied to the mechanism, its motion from an arbitrary initial state to the given final state can be provided.

In [7] controllable rectilinear motion along a rough surface of the system of two bodies interacting with each other via the control force was studied. In [13, 14] the rectilinear motion along a horizontal rough surface of the body with the moving internal mass which also moves along the straight line parallel to the line of motion of the body was addressed. The asymmetry of the friction force necessary for motion in the given direction is provided by the dependence of the friction coefficient on the sign of the velocity of the constituent bodies of the system.

In [15] the dynamics of the mobile system including two bodies connected by an elastic element with the linear characteristic were analyzed. The motion was excited by the harmonic force acting between the bodies.

In [16, 17] the dynamics of motion of worm-like robots for the cases with infinite and finite number of bodies was discussed.

In [18–20] the mathematical model was developed and the motion of the two-mass system was studied with account of characteristics of the electric drive. In this system one mass directly contacted the rough surface, while the second mass moved with respect to the first mass without friction.

In [21] the dynamics of controlled vibration-driven and vibroimpact motion of a mobile system were addressed.

1. DESCRIPTION OF A MOBILE VIBRATION-DRIVEN SYSTEM

In this paper, the behavior of the two-mass vibration-driven system including two solid bodies connected by the piecewise linear viscous–elastic element and the electromagnetic drive is studied; both bodies contact with the rough surface. Under the action of the electromagnetic drive, the bodies perform the vibration-driven motion. For obtaining the translational motion of the robot along the rough surface each body is equipped with the device which provides its displacement in one direction only. This effect can be achieved, for example, by equipping the contact surfaces of the robot with special flake-like (needle-like) plates with the required flake (needle) orientation. The asymmetry of friction forces can also be obtained by applying special controllable friction mechanisms.

The schematic diagram of the system is shown in Fig. 1. System masses *1* and *4* are connected with each other by elastic element *6*. Each body is equipped with mechanisms *5*, which provide the asymmetry of the friction force between the masses and the bearing surface. The electromagnetic drive consists of a core with

the coil *2* installed on body *1* and anchor *3* attached to body *4*.

The system moves due to the periodic approach of the bodies under the action of the force of the electromagnetic drive. In this case body *1* approaches body *4* which stops due to the presence of asymmetric mechanism *5*. After electric power is switched off, body *4* goes away from body *1* under the action of spring *6*; body *1*, in turn, remains in its place due to the action of its mechanism *5*. Thus, the center of mass of the system moves. This motion principle was described in [22].

2. MATHEMATICAL MODEL OF A MOBILE VIBRATION-DRIVEN SYSTEM

The numerical scheme of the studied system is shown in Fig. 2. The following notation is used: X_1 and X_2 are the generalized coordinates, ΔX is the length of the elastic–viscous limiter, Δ is the distance between the masses in the case of the undeformed spring; Λ is the distance between the masses under deformed spring; C, μ, C_2, μ_2 are the stiffness and the viscosity coefficients of the spring and the elastic–viscous limiter. The following forces act on the mass m_1: Q_1 of the electromagnetic drive, P_1 of the elastic element, R_1 of resistance. The following forces act on the mass m_2: Q_2, P_2, and R_2. Obviously, the absolute values of these forces are pairwise equal and their signs are opposite. Along with these forces, dry friction forces F_1 and F_2 act on the masses m_1 and m_2.

The periodic forces Q_1 and Q_2 serve as the driving action; these forces are internal and cause the vibration-driven motion of the masses m_1 and m_2 with respect to the center of mass of the system. The motion of the center of mass takes place because the friction forces applied to masses *1* and *4* are external and have different absolute values depending on the velocity direction, which results in the occurrence of the translational motion of the robot in the positive direction of the axis *OX*.

Let us write the differential equations describing the motion of the system masses:

$$\begin{aligned} m_1\ddot{X}_1 &= -P_1 - R_1 + F_1 - Q_1, \\ m_2\ddot{X}_2 &= P_2 + R_2 + F_2 + Q_2 \end{aligned}. \qquad (2.1)$$

Here, dots denote the time derivatives of the generalized coordinates. If these equations are summed, we obtain the motion equations of the center of mass of the studied system

$$m_1\ddot{X}_1 + m_2\ddot{X}_2 = F_1 + F_2,$$

since

$$m_1\ddot{X}_1 + m_2\ddot{X}_2 = m\ddot{X}_c,$$

we have

$$m\ddot{X}_c = F_1 + F_2, \qquad (2.2)$$

where $m = m_1 + m_2$ is the system mass, and X_c is the coordinate of the center of mass of the system.

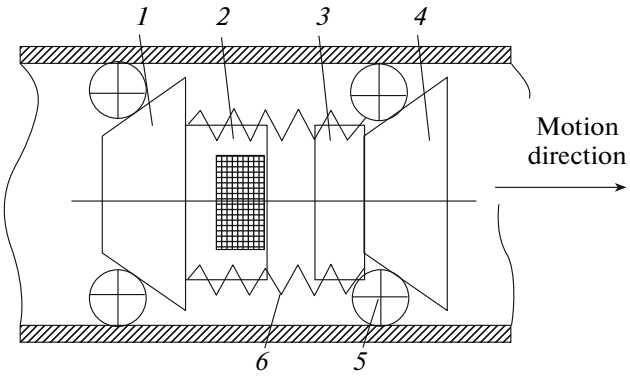

Fig. 1. Schematic diagram of the mobile two-mass vibration-driven system.

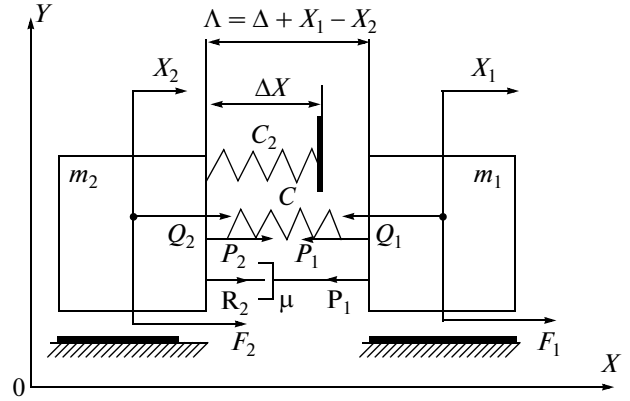

Fig. 2. Numerical scheme of the mobile vibration-driven system.

In the considered scheme the elastic element is piecewise linear with the parameters C, μ, C_2, and μ_2. Let us construct the model of the elastic force. It can be seen from Fig. 3 that the additional spring with the stiffness C_2 is included in the operation depending on the distance between the masses Λ and ΔX. The value of Λ is determined as

$$\Lambda = \Delta + X_1 - X_2. \qquad (2.3)$$

If $\Lambda > \Delta X$ then only the spring with the stiffness C is deformed, and the shock-free mode of motion is realized. In the opposite case, if $\Lambda < \Delta X$, the step-like stiffness correction takes place which results in the fast change of the velocity of the masses m_1 and m_2; therefore, this motion can be considered vibroimpact.

The model of the elastic force is represented as

$$P_1 = \begin{cases} C(X_1 - X_2), & \text{if } \Lambda > \Delta X, \\ C(X_1 - X_2) + C_2(\Delta + X_1 - X_2 - \Delta X), \\ \Lambda < \Delta X, \end{cases} \qquad (2.4)$$

$$P_2 = -P_1.$$

Figure 3 shows the dependences of the elastic forces P_1 and P_2 on the distance between the masses Λ.

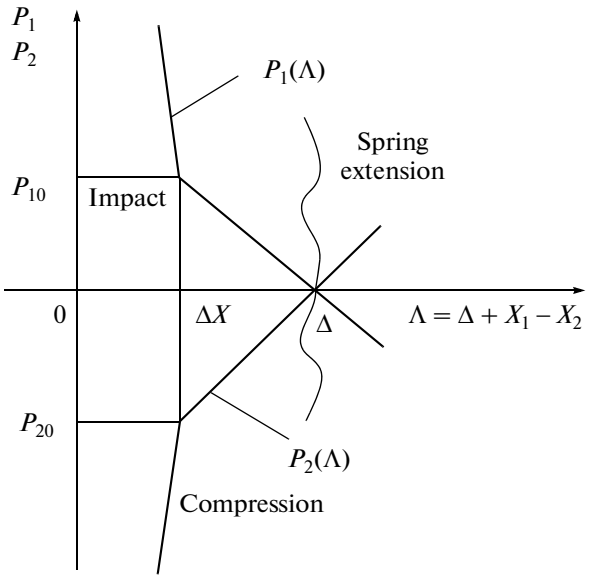

Fig. 3. Elastic force as a function of the distance between masses.

For $\Lambda = \Delta$ the elastic forces are equal to zero. If $\Lambda = \Delta X$, the mass m_1 contacts the spring C_2; in this case, the elastic forces are P_{10} and P_{20}. Further reduction of Λ results in the step-like change of the total stiffness of the elastic element.

The model of the force of viscous resistance is described as

$$R_1 = \begin{cases} \mu(V_1 - V_2), & \text{if } \Lambda > \Delta X, \\ \mu(V_1 - V_2) + \mu_2(V_1 - V_2), & \Lambda < \Delta X, \end{cases} \qquad (2.5)$$
$$R_2 = -R_1.$$

Here, μ is the viscous resistance coefficient, $V_i = dX_i/dt$ are the velocities of the masses m_1 and m_2.

Let us take the model of the friction force in the following form:

$$F_i = \begin{cases} F_i, & \dot{X}_i < 0; \\ 0, & \dot{X}_i > 0; \\ F_i^*, & \dot{X}_i = 0, \end{cases} \qquad (2.6)$$

where F_i^* is the static friction force determined from the condition of equilibrium of forces acting on the motionless ith mass, $\dot{X}_i$ is the velocity of the ith mass.

The forces acting on the masses from the electromagnetic drive are calculated using the formula

$$Q_1 = -Q_2 = \frac{\Phi^2}{\mu_0 S z^2}. \qquad (2.7)$$

In this expression Φ is the magnetic flux in the magnetic circuit of the core, μ_0 is the magnetic permittivity, S is the area of the air gap, and z is the number of coils of the conductor with flowing current. For representation of the magnetic flux Φ we use the following equation:

$$\dot{\Phi} + rI = u(t), \qquad (2.8)$$

which establishes the connection between the electric power voltage $u(t)$, the magnetic flux Φ, the current I, and the active resistance of the electromagnet coil r.

The current flowing in the electric circuit is determined as

$$I = \frac{\partial \mathrm{W}}{\partial \Phi}, \text{ where } W = \frac{\Phi^2}{2\mu_0 S z^2}.$$

Then

$$I = \frac{\Phi\Lambda}{\mu_0 S z}. \qquad (2.9)$$

Let us consider the case of when the periodic electric voltage with the amplitude U_0 and the frequency ω is applied to the coil. According to the connection scheme, the voltage $u(t)$ is simulated as

$$u(t) = \begin{cases} U_0 \sin(\omega t), & \text{if } u(t) > 0, \\ 0, & \text{if } u(t) < 0. \end{cases}$$

The system of equations describing the dynamics of motion of the center of mass of the vibration-driven system has the form

$$\begin{cases} \dot{\hat{O}} + \dfrac{2r(\Delta + X_1 - X_2)}{Sz\mu_0}\hat{O} = u(t), \\ m_1\ddot{X}_1 = P_1 + R_1 + F_1 + Q_1, \\ m_2\ddot{X}_2 = P_2 + R_2 + F_2 + Q_2. \end{cases} \qquad (2.10)$$

Let us represent the dimensional variables included in system of equations (2.10) in the dimensionless form, introducing the following notation:

$$\tau = \omega t, \quad X = X_0\bar{X},$$
$$\dot{X} = X_0\omega\dot{\bar{X}}, \quad \ddot{X} = X_0\omega^2\ddot{\bar{X}}, \qquad (2.11)$$
$$\bar{u}(\tau) = U_0\bar{u}(t), \quad \Phi = \Phi_0\bar{\Phi},$$

where τ is the dimensionless time, X_0 is the length scale, U_0 is the electric voltage scale, and Φ_0 is the flux scale. The barred variables are dimensionless.

System of differential equations (2.10) with account of (2.11) in the dimensionless form is written as

$$\begin{cases} \dot{\bar{\Phi}} = E\bar{u}(\tau) - \beta\cdot(\bar{\Delta} + (\bar{X}_1 - \bar{X}_2))\bar{\Phi}, \\ \ddot{\bar{X}}_1 = -\bar{R}_1 - \bar{P}_1 - \chi\bar{\Phi}^2 + \bar{F}_1, \\ \ddot{\bar{X}}_2 = \bar{m}\bar{R}_2 - \bar{P}_2 + \bar{m}\chi\bar{\Phi}^2 + \bar{m}\bar{F}_2. \end{cases} \qquad (2.12)$$

Here, the following notation is used:

$$\bar{P}_1 = \begin{cases} \xi(\bar{X}_1 - \bar{X}_2), & \bar{\Lambda} > \Delta\bar{X}; \\ \xi(\bar{X}_1 - \bar{X}_2) + \alpha\xi(\bar{\Delta} - \Delta\bar{X} + \bar{X}_1 - \bar{X}_2), \\ \bar{\Lambda} \le \Delta\bar{X}; \end{cases}$$

$$\bar{P}_2 = \begin{cases} \bar{m}\xi(\bar{X}_1 - \bar{X}_2), & \bar{\Lambda} > \Delta\bar{X}; \\ \bar{m}\xi(\bar{X}_1 - \bar{X}_2) + \bar{m}\alpha\xi(\bar{\Delta} - \Delta\bar{X} + \bar{X}_1 - \bar{X}_2), \\ \bar{\Lambda} \le \Delta\bar{X}; \end{cases}$$

$$\bar{R}_1 = \begin{cases} \xi(\dot{\bar{X}}_1 - \dot{\bar{X}}_2), & \bar{\Lambda} > \Delta\bar{X}; \\ \xi(\dot{\bar{X}}_1 - \dot{\bar{X}}_2) + \alpha\xi(\dot{\bar{X}}_1 - \dot{\bar{X}}_2), & \bar{\Lambda} \le \Delta\bar{X}; \end{cases}$$

$$\bar{R}_2 = \begin{cases} \bar{m}\xi(\dot{\bar{X}}_1 - \dot{\bar{X}}_2), & \bar{\Lambda} > \Delta\bar{X}; \\ \bar{m}\xi(\dot{\bar{X}}_1 - \dot{\bar{X}}_2) + \bar{m}\alpha\xi(\dot{\bar{X}}_1 - \dot{\bar{X}}_2), & \bar{\Lambda} \le \Delta\bar{X}; \end{cases} \quad (2.13)$$

$$E = \frac{U_0}{\Phi_0\omega}; \ \beta = \frac{2X_0 r}{\mu_0 S\omega}; \ \xi = \frac{C}{\omega^2 m_1} = \frac{\lambda_1^2}{\omega^2};$$

$$\chi = \frac{(\Phi_0)^2}{\mu_0 S z^2 X_0 \omega^2 m_1}; \quad \bar{m} = \frac{m_1}{m_2};$$

$$\bar{\Delta} = \frac{\Delta}{X_0}; \quad \varsigma\zeta = \frac{\mu}{m_1\omega}; \quad \alpha = \frac{C}{C_1}; \quad \Delta\bar{X} = \frac{\Delta X}{X_0}.$$

The dimensionless parameters $E, \beta, \xi, \chi, \alpha, \zeta, \bar{m}, \bar{\Delta}$, and $\Delta\bar{X}$ determine the law of the system motion. The parameter β characterizes the electric dissipative properties of the electromagnetic drive, ζ depends on the losses in the elastic-viscous element. The parameter ξ is determined by the ratio of the squared partial frequency of the first mass of the system and the squared frequency of external action. The parameter χ determines the amplitude of the electromagnetic force, $\bar{m}$ is the parameter representing the ratio of the system masses, and $\bar{\Delta} - \bar{\Delta}x$ is the dimensionless gap between the masses calculated for the undeformed spring position.

3. RESULTS OF SIMULATION OF MOTION OF A VIBRATION-DRIVEN SYSTEM

Let us study the influence of the parameters ξ, $\bar{m}$, and E on the average velocity of established motion of the system. The other parameters are assumed to be constant.

The electric voltage applied to the coil varies according to the law shown in Fig. 4.

At the first stage the modes of the system motion for which $\Lambda > \Delta X$ are studied; this corresponds to the case when the masses do not collide. Equations (2.10) are solved numerically; the algorithm is based on the Euler method with the adaptive integration step.

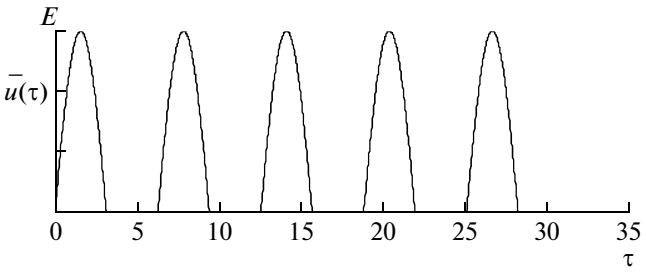

Fig. 4. Electric voltage applied to the coil winding.

It is known [23] that eigenfrequencies of the linear two-mass system in the absence of resistance forces are determined using the formula

$$p_{1,2}^2 = \frac{1}{2}\left(\lambda_1^2 + \lambda_2^2\right) \mp \sqrt{\frac{1}{4}\left(\lambda_1^2 - \lambda_2^2\right)^2 + \frac{m_1}{m_2}\lambda_2^4}, \quad (3.1)$$

where λ_1 and λ_2 are the partial parameters:

$$\lambda_1 = \sqrt{\frac{c}{m_1}}, \quad \lambda_2 = \sqrt{\frac{c}{m_2}}.$$

Figure 5 shows the dependences of the average velocity of the established motion of the robot on the parameter ξ for four values of the electric power amplitude E for $\bar{m} = 1.0$. The analysis of these dependences demonstrated that in the region $\xi = 0.5$ the sharp increase in the average velocity of the system is observed. This corresponds to the main resonance of the considered system which takes place if the eigenfrequency coincides with the frequency of the external action $p = \omega$. Since $\bar{m} = 1$, we have $\lambda_1 = \lambda_2$. Then taking into account (2.3), (2.4) we obtain $p_1^2 = 0$, $p_2^2 = 2\lambda_1^2$. The second peak of the velocity growth takes place for $\xi = 2$ due to the resonance under the condition $p = 2\omega$. The third peak corresponds to the condition $p = 3\omega$ or $\xi = 4.5$. The maximal value of the average velocity obtained for shock-free modes is in the narrow region of the first resonance, it is equal to 0.225.

The studies demonstrated that further increase in the electric voltage amplitude results in the fact that the system passes the mode of vibroimpact mass interaction. For $E = 8$ shock modes are observed in the region of the first resonance; these modes are accompanied by small expansion of the first resonance region. In this case, the value of the average velocity reaches approximately 0.4, which exceeds by almost a factor of 2 the maximal velocity for the shock-free mode.

As the electric voltage level is further increased (see Fig. 6 for a dimensionless mass of 1.35), the region with high average velocity extends. Thus, for the power voltage $E = 11$ the high velocity region occurs near the second resonance. If E increases to 14, we have a sufficiently broad frequency region $\xi = 0.5$–2.5 in which

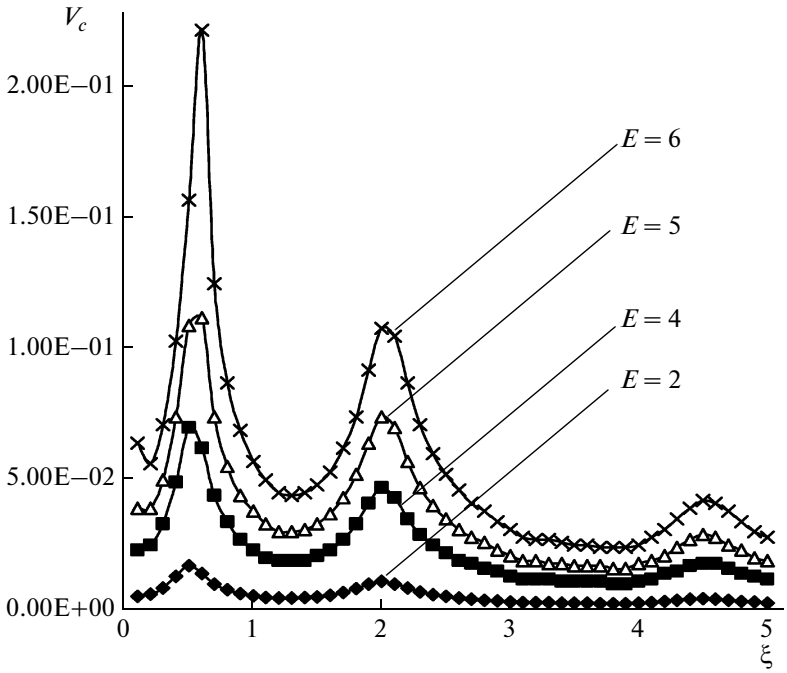

Fig. 5. Average velocity V_c of the vibration-driven robot as a function of the dimensionless parameter ξ for different electric power levels.

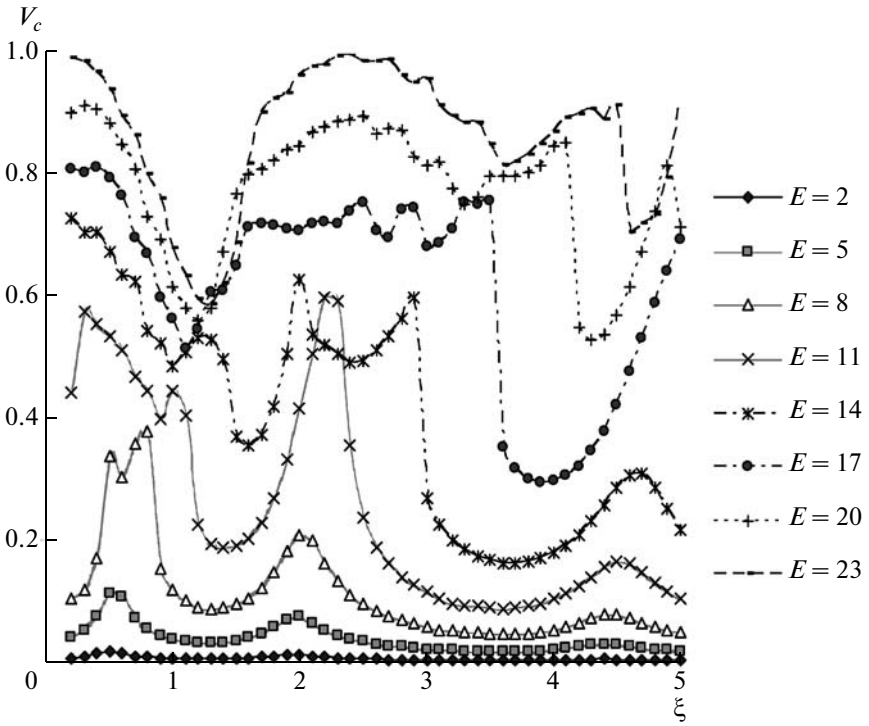

Fig. 6. Average velocity V_c of the vibration-driven robot as a function of the dimensionless parameter ξ for different electric power levels (the levels are indicated in the table on the right-hand side, $\bar{m} = 1.05$).

the average velocity of the system corresponds to the high level $V_c = 0.55–0.65$ and remains practically constant. Further increase in E up to 17 results in even stronger extension of the high velocity region. In the frequency region $\xi = 1.25–3.5$, where $V_c = 0.7–0.9$. The maximal average velocity is observed for $E = 23$,

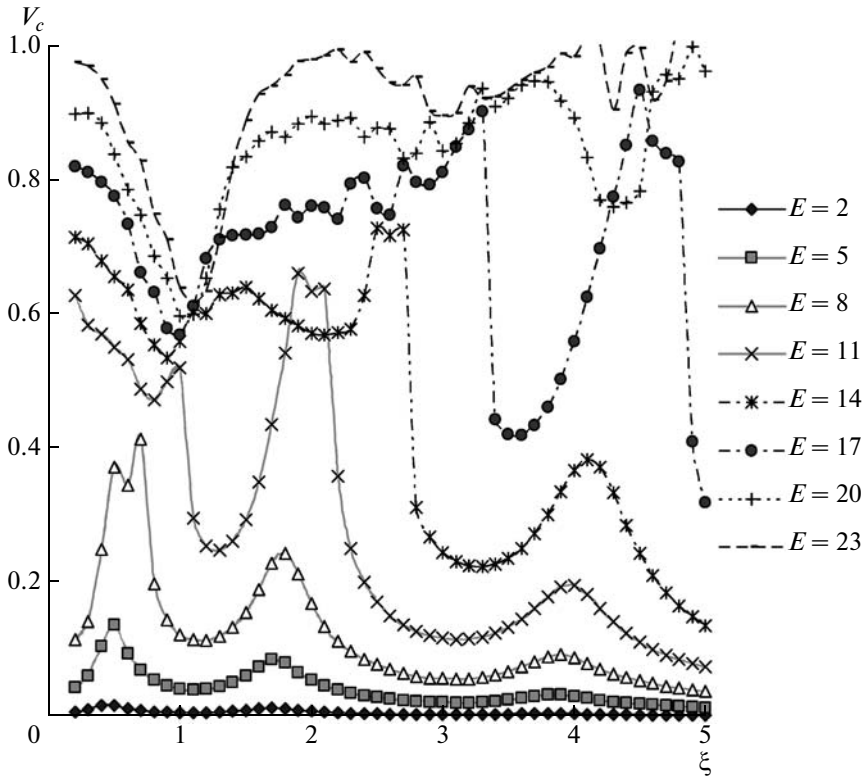

Fig. 7. Average velocity V_c of the vibration-driven robot as a function of the dimensionless parameter ξ for different electric power levels (the levels are indicated in the table on the right-hand side, $\bar{m} = 1.35$).

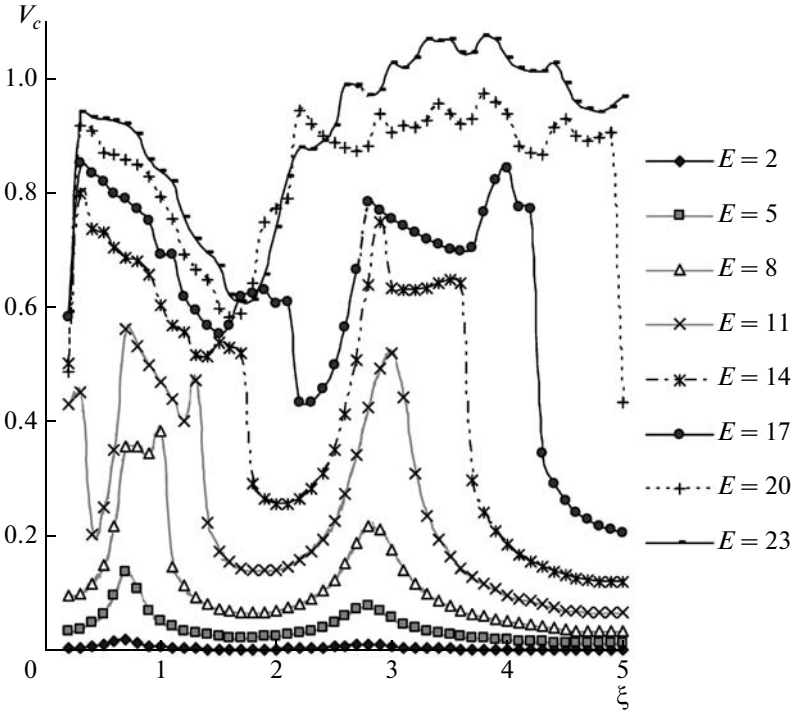

Fig. 8. Average velocity V_c of the vibration-driven robot as a function of the dimensionless parameter ξ for different electric power levels (the levels are indicated in the table on the right-hand side, $\bar{m} = 0.45$).

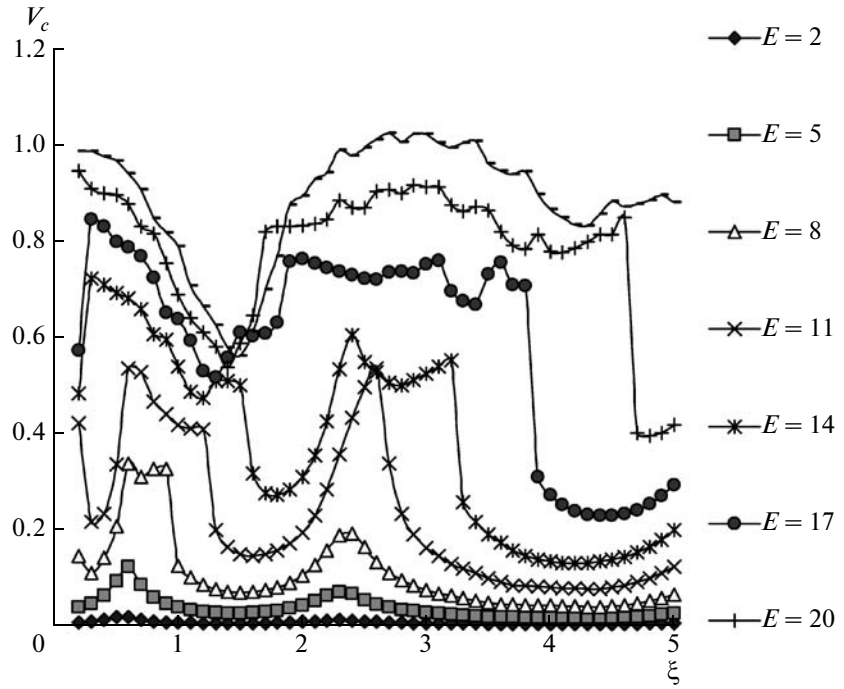

Fig. 9. Average velocity V_c of the vibration-driven robot as a function of the dimensionless parameter ξ for different electric power levels (the levels are indicated in the table on the right-hand side, $\bar{m} = 0.75$).

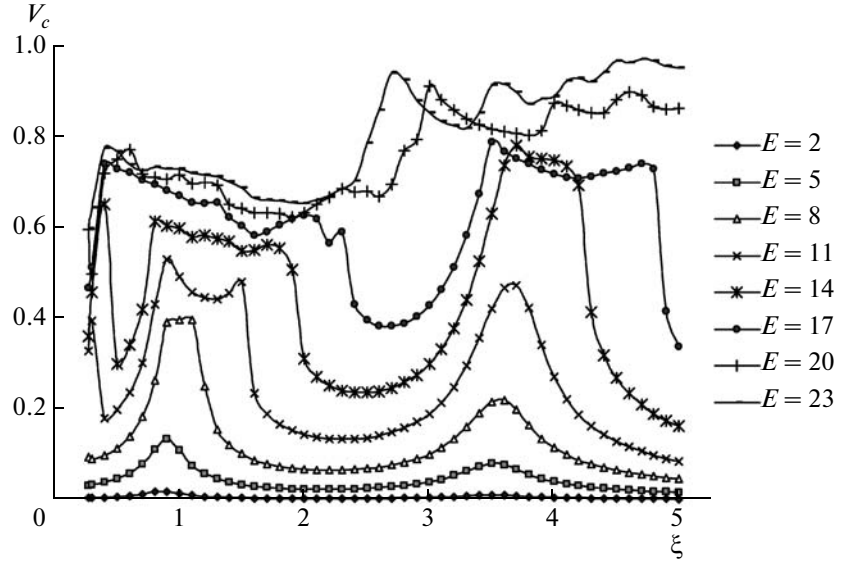

Fig. 10. Average velocity V_c of the vibration-druven robot as a function of the dimensionless parameter ξ for different electric power levels (the levels are indicated in the table on the right-hand side, $\bar{m} = 0.15$).

and in the broad frequency range $\xi = 1.5$–4.0 the velocity is within $V_c = 0.9$–1.0. At the same time, the region in which the system velocity decreases, i.e., a kind of a "dip", is observed near $\xi = 1$.

The velocity decreases in a similar way in the high frequency region depending on the electric power amplitude; thus, for $E = 14$ the velocity drops for the dimensionless frequency higher than $\xi = 3$. For $E = 17$ the velocity decreases for $\xi = 3.5$, and for $E = 20$, for $\xi = 3.8$. For the power voltage $E = 23$ the sharp velocity drop begins for $\xi = 4.2$.

Similar results were obtained for the dimensionless mass $\bar{m} = 1.05$ (Fig. 7), $\bar{m} = 0.45$ (Fig. 8), $\bar{m} = 0.75$ (Fig. 9), and $\bar{m} = 0.15$ (Fig. 10).

CONCLUSIONS

The two-mass vibration-driven system in the presence of the asymmetric dry friction at the mass–rough surface contact moves along the surface with the average velocity depending on the frequency and amplitude of the control voltage, and on the mass ratio. In the region of shock-free modes the dimensionless frequency ξ strongly influences the average velocity of the established motion of the system. The velocity dependence on the dimensionless parameter ξ takes place. Modes with sharp increase in the average velocity for some values of ξ are observed. Depending on the value of ξ the system masses move along different trajectories. In the region $\xi = 0.5$ the masses oscillate oppositely with the frequency of the external periodic action, for $\xi = 2.0$ the masses vibrate with the doubled frequency; in this case the average system mass considerably decreases. With increasing electric power amplitude E the system is switched to the vibroimpact motion mode, which results in the considerable increase in the average velocity and extension of the frequency range in which high velocities are provided.

ACKNOWLEDGMENTS

This work was supported by the Russian Foundation for Basic Research, project nos. 08-08-000438-a and 09-01-91339_NNIO_a.

REFERENCES

1. F. L. Chernous'ko, "Multilink Robot Motion on a Horizontal Plane", Appl. Math. Mech., **64** (1), 8–18 (2000).
2. F. L. Chernous'ko, "Wave-Like Multilink Robot Motion on a Horizontal Plane", Appl. Math. Mech., **64** (4), 5–15 (2000).
3. F. L. Chernous'ko, "Plane Multilink Robot Motion on a Rough Horizontal Plane", Dokl. Akad. Nauk, **370** (2), 186–189 (2000).
4. F. L. Chernous'ko, "ThreeLink Robot Motion on a Plane", Appl. Math. Mech., **65** (1), 15–20 (2001).
5. F. L. Chernous'ko, "Controlled Two-Link Robot Motion on a Horizontal Plane", Appl. Math. Mech., **65** (4), 578–591 (2001).
6. A. S. Smyshlyaev and F. L. Chernous'ko, "Optimization of the Motion of Multilink Robots on a Horizontal Plane", Izv. Ross. Akad. Nauk, Teor. Sist. Upr., no. 2, 176–184 (2001) [Comp. Syst. Sci. **40** (2), 340–348 (2001)].
7. F. L. Chernous'ko, "Optimal Rectilinear Motion of a Two-Mass System", Appl. Math. Mech., **66** (1), 3–9 (2002).
8. F. L. Chernous'ko, "Snake-Like Locomotions of Multilink Mechanisms", Vibr. Contr., **9** (1–2), 235–256 (2003).
9. T. Yu. Figurina, "Quasistatic Motion of a Two-Link Robot on a Horizontal Plane", Izv. Ross. Akad. Nauk, Mekh. Tverd. Tela, **1**, 31–41 (2003).
10. T. Yu. Figurina, "Controlled Quasistatic Motions of a Two-Link Robot on a Horizontal Plane", Izv. Ross. Akad. Nauk, Teor. Sist. Upr., no. 3, 160–176 (2004) [Comp. Syst. Sci. **43** (3), 481–496 (2004)].
11. T. Yu. Figurina, "Quasi-Static Motion of a Two-Link System along a Horizontal Plane", Multibody System Dynamics, **11** (3), 251–272 (2004).
12. T. Yu. Figurina, "Controlled Slow Motions of a Three-Link Robot on a Horizontal Plane", Izv. Ross. Akad. Nauk, Teor. Sist. Upr., no. 3, 149–156 (2005) [Comp. Syst. Sci. **44** (3), 473–480 (2005)].
13. F. L. Chernous'ko, "Motion of a Body with Mobile Internal Mass", Dokl. Akad. Nauk, **405** (1), 1–5 (2005).
14. F. L. Chernous'ko, "Analysis and Optimization of Motion of a Body Controlled via a Mobile Internal Mass", Appl. Math. Mech., **70** (6), 915–941 (2006).
15. K. Zimmerman, I. Zeidis, and M. Pivovarov, "Dynamics of a Nonlinear Oscillator in Consideration of Nonsymmetric Coulomb Dry Friction" in *Proceedings of 5th Euromechanics Nonlinear Dynamics Conference, Book of Abstracts, Eidnhoven, Netherlands, 2005*, p. 308.
16. K. Zimmerman, I. Zeidis, J. Steigenberger, et al., "An Approach to the Modelling of Worm-Like Motion Systems with a Finite Number of Degrees of Freedom", in *Proceedings of 4th International Conference on Climbing and Walking Robots "First Steps in Technical Realization" Karlsruhe, Germany, 2001*, pp. 561–568.
17. K. Zimmerman, I. Zeidis, and J. Steigenberger, "Mathematical Model of Worm-Like Motion Systems with Finite and Infinite Numbers of Degrees of Freedom", in *Proceedings of 14th CISM IFToMM Symposium on Theory and Practice of Robots and Manipulators, 2002*, pp. 7–16.
18. S. F. Yatsun, P. A. Bezmen, and Yu. Yu. Losev, *Mathematical Simulation of Motion of a Vibration-Driven Mobile Robot with Internal Mobile Mass* (Kursk Gos. Universitet, Kursk, 2008) [in Russian].
19. S. F. Yatsun, V. Ya. Mishchenko, and A. V. Razin'kova, "Pulsed Vibration-Driven Mover", RF Patent for Useful Model no. 66433 (14.09.2007).
20. N. N. Bolotnik, I. M. Zeidis, K. Zimmerman, and S. F. Yatsun, "Dynamics of Controlled Motion of Vibration-Driven Systems", Izv. Ross. Akad. Nauk, Teor. Sist. Upr., no. 5, 157–167 (2006) [Comp. Syst. Sci. **45** (5), 831–840 (2006)].
21. A. N. Grankin and S. F. Yatsun, "Investigation of Vibroimpact Regimes of Motion of a Mobile Microrobot with Electromagnetic Drive", Izv. Ross. Akad. Nauk, Teor. Sist. Upr., no. 1, 163–171 (2009) [Comp. Syst. Sci. **48** (1), 155–164 (2009)].
22. V. G. Chashchukhin, "Simulation of Dynamics and Determination of Control Parameters of Inpipe Minirobot", Izv. Ross. Akad. Nauk, Teor. Sist. Upr., No. 5, 142–147 (2008) [Comp. Syst. Sci. **47** (5), 806–811 (2008)].
23. K. Magnus, *Oscillations* (Mir, Moscow, 1982) [in Russian].